Climate Dynamics (2004) 22: 447–459
DOI 10.1007/s00382-003-0387-4

W. C. Chao · B. Chen

Single and double ITCZ in an aqua-planet model with constant sea surface temperature and solar angle

Received: 17 June 2003 / Accepted: 5 December 2003 / Published online: 16 March 2004

Abstract It has been known for more than a decade that an aqua-planet model with a globally- and temporally-uniform sea surface temperature and solar isolation angle can generate intertropical convergence zones (ITCZ). Employing such a model, previous studies have shown that one of several means can be used to change between a single ITCZ over the equator and a double ITCZ straddling the equator. These means include switching to a different cumulus parametrization scheme, making changes within the cumulus parametrization scheme, and changing other aspects of the model such as horizontal resolution. Here, an interpretation of these findings is offered. In an aqua-planet model with globally and temporally uniform sea surface temperature and solar isolation angle, the latitudinal location of an ITCZ is the latitude where a balance exists between two types of attraction, both resulting from the Earth's rotation. The first attraction pulls the ITCZ towards the equator and is not sensitive to changes in model design. It is directly related to the Coriolis parameter, which provides stability to the atmosphere. The second ssattraction pulls the ITCZ poleward and *is* sensitive to changes in model design. It is related to the convective circulation, modified by the Coriolis force. A balance between the two types of attraction is reached either at the equator or more than 10° north and south of the equator, depending on the shape and magnitude of the attractions. A balance at the equator yields a single ITCZ over the equator, whereas a balance north and south of the equator yields a double ITCZ straddling the equator.

W. C. Chao (✉)
Laboratory for Atmospheres, Mail code 913,
NASA/Goddard Space Flight Center,
Greenbelt, MD 20771, USA
E-mail: winston.c.chao@nasa.gov

B. Chen
GEST Center, University of Maryland,
Baltimore County, USA

1 Introduction

The intertropical convergence zone (ITCZ) is a prominent component of the general circulation of the atmosphere. In this study the ITCZ is equated with the regions of maximum time-mean (e.g., monthly mean) precipitation in the tropics. The origin of the ITCZ, including its latitudinal location, has attracted the attention of many researchers (e.g., Charney 1971; other references cited in the Appendix), because it is not only theoretically interesting, but has practical application as well. For example, a good simulation of the ITCZ is important for the simulation of surface winds in the equatorial regions, which, in turn, is crucial for the simulation of El Nino using coupled ocean–atmosphere models. The current atmospheric general circulation models (GCMs) have considerable difficulties in getting a good simulation of the ITCZs, in terms of both their locations and intensity. Therefore, this topic (the origin of the ITCZ, including its latitudinal location) has remained an active area of research.

The peak in the latitudinal profile of sea surface temperature (SST) plays a fundamental role in determining the latitudinal location of the ITCZ; however, it is not predominant. Figure 1 shows the August climatology of the SST (C) and precipitation (mm/day) in the Indian Ocean and western Pacific region. It shows that maximum precipitation does not coincide with maximum SST. For example, in the equatorial region between 60°E and 75°E, although the latitudinal peak of the SST is in the northern Indian Ocean, there is a latitudinal peak of precipitation in the southern Indian Ocean. Therefore, other factors clearly play important roles in determining the latitudinal location of the ITCZ.

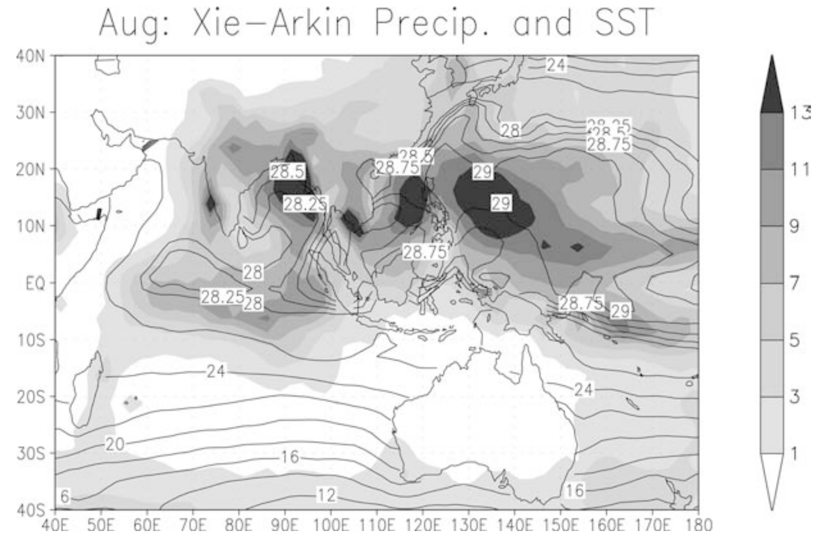

Fig. 1 August Xie-Arkin precipitation (mm/day) and sea surface temperature (contour lines in °C) in Indian Ocean and western Pacific region averaged from 1979 to 1998

In this study, the focus is on these other factors. They include the Earth's rotation, the interaction between convection and radiation, and the interaction between convection and surface fluxes. Because convection is at the center of the problem, it is expected that in a general circulation model the cumulus convection scheme plays a role in determining the latitudinal location of the ITCZ. The central goal of this investigation is to ascertain how these factors play their roles. Our approach is to rely on experiments with an aqua-planet model with globally uniform SST and solar angle. This simplified setting excludes the roles of SST variation and solar angle change, and allows us to concentrate on other important factors. Thus, what we are studying is a subset of ITCZ research.

It has been known for more than a decade from numerical simulation, that the Earth's rotation alone, without an equator-to-pole gradient in radiative-convective equilibrium temperature, is sufficient to give rise to an intertropical convergence zone (ITCZ) and atmospheric general circulation (Sumi 1992; Kirtman and Schneider 2000). Although this simulated general circulation is considerably different from the observed general circulation (for example, the Hadley circulation is much weaker than what is observed), it is a useful tool to gain insight into some basic mechanisms governing atmospheric general circulation and the ITCZ in particular.

Aqua-planet models with globally and temporally uniform SST and solar angle (U-SST-SA), which have no equator-to-pole gradient in radiative-convective equilibrium temperature, have been used by many researchers. Sumi (1992) used such a model to study the effects of evaporation rate and the Earth's rate of rotation on the organization of convective activities. In Sumi's (1992) study, the Kuo (1965) cumulus parametrization was used. He found, among other things, that by merely doubling horizontal resolution, a single ITCZ at the equator turned into a double ITCZ straddling the equator. Sumi (1992) interpreted this result as a consequence of the low-resolution model's not having sufficient resolution to resolve the double ITCZ, with a single ITCZ being the result. We will discuss this interpretation. Sumi (1992) also found that by switching to Manabes et al. (1965) moist convective adjustment scheme (MCA), the double ITCZ remains. (Note: Sumi 1992 did not use a constant solar angle, but used a globally-uniform net radiative cooling rate.)

Hess et al. (1993) also found sensitivity of the ITCZ to the cumulus convection scheme in an aqua-planet model with a latitudinal-varying SST. Kirtman and Schneider (2000) also did an experiment similar to that of Sumi's (1992), but with the relaxed Arakawa-Schubert scheme (hereafter, RAS Moorthi and Suarez 1992), and obtained a single ITCZ over the equator. On the other hand, our similar experiments with the same scheme gave a double ITCZ (Chao 2000). We also found that switching to MCA can turn a double ITCZ into a single ITCZ over the equator (Chao 2000). (This is different from Sumi 1992 results and indicates that factors other than the convection scheme also matter. Exactly what these other factors are remains unknown.) Furthermore, our experiments revealed that by imposing on RAS a condition of the boundary layer relative humidity being greater than a critical value before RAS is allowed to function at each grid, and through increasing this critical value, RAS can be made to behave like MCA in the sense that a double ITCZ can be switched to a single ITCZ over the equator (Chao and Chen 2001a, hereafter CC01). Sometimes, only one component of the double ITCZ appears as an off-equatorial ITCZ; this is still distinct from the single ITCZ over the equator (Chao 2000, CC01).

In summary, previous studies have shown that one of several model design changes can induce the ITCZ in an aqua-planet model under the U-SST-SA conditions to change between a single ITCZ at the equator and a double ITCZ straddling the equator. These model design changes include switching to a different cumulus parametrization scheme, making changes within the cumulus parametrization scheme, and making changes in other aspects of the model such as horizontal resolution. Sometimes, only one component of a double ITCZ shows up; even so, this is an ITCZ away from the equator, quite distinct from a single ITCZ over the equator. The study of the modeled ITCZ under U-SST-SA conditions, as a subset of the study of the modeled ITCZ, has the advantage of removing the effects of spatial variation of the SST and solar angle and the effects of ocean–atmosphere interaction. This allows the roles of the Earth's rotation, cumulus convection, and other factors to be studied in isolation. CC01 made an initial attempt to explain the findings from such studies based on the concept of rotational ITCZ attractors, which they introduced; however, not all findings were explained. For example, CC01 showed that by modifying RAS, the latitude of the ITCZ under U-SST-SA conditions can switch between an equatorial and an off-equatorial location. They also showed that the speed of the switch from an equatorial to an off-equatorial location is much faster than in the reverse direction (reproduced here as Figs. 2 and 3; details to be explained). These experimental results were not explained in CC01. Thus, one of our purposes is to offer further interpretation. The difficulties that these experimental findings have posed for previous theories of latitudinal location of the ITCZ are set forth in the Appendix.

2 Experiments and interpretations

To understand the model results mentioned in the introduction, experiments are conducted using the Goddard Earth Observing System atmospheric general circulation model (GEOS-version 2, Takacs et al. 1994), employing the simplified settings of an aqua-planet. A brief description of the model can be found in CC01. This is a latitude-longitude (4° × 5°) grid model with 21 vertical levels.

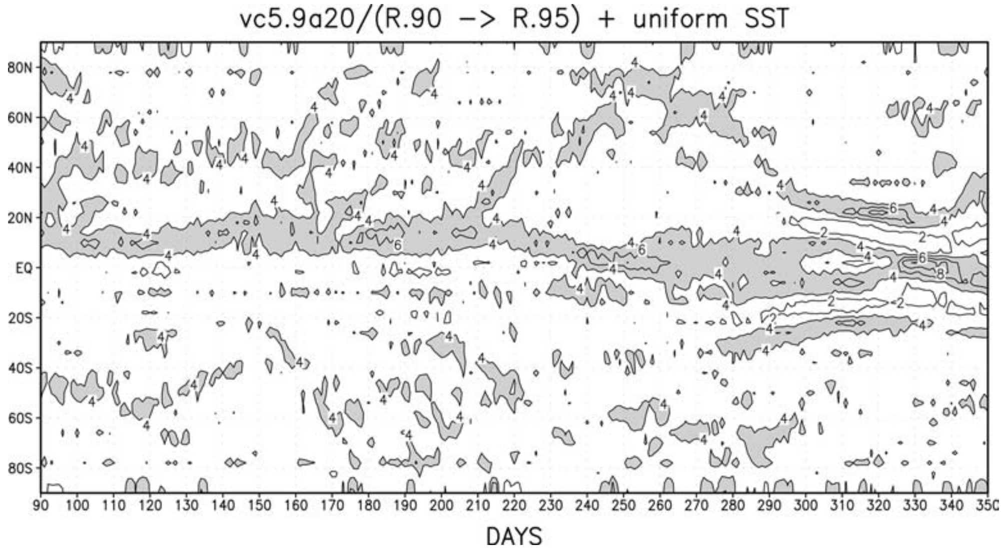

Fig. 2 Zonally averaged precipitation (mm/day) as a function of time in an experiment with uniform SST and solar insolation with a condition that for cumulus convection to occur the boundary layer relative humidity has to be greater than a critical value. The critical value is 90% in the first 200 days and then increased linearly in time in the next 100 day to 95%

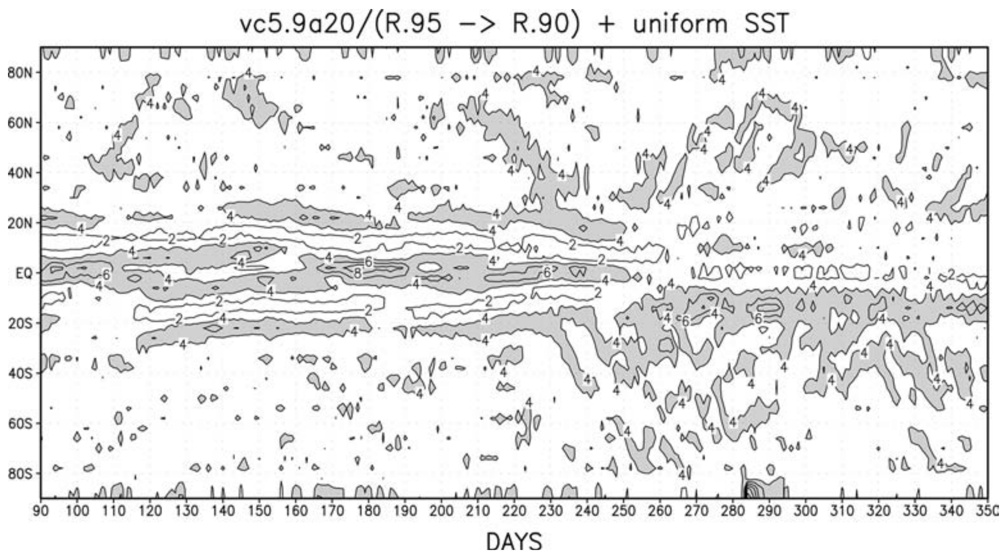

Fig. 3 Same as Fig. 2 except that the values of 90% and 95% are switched

A prominent feature of the model is its use of the relaxed Arakawa-Schubert cumulus scheme (RAS). The model's ability to simulate the ITCZ in a realistic setting is demonstrated in Fig. 1b of Chao and Chen (2001b). The model captures the gross features of the monthly mean precipitation patterns. However, there are many problems in the details, as with all GCMs.

The experimental strategy is to start with the simplest model settings and gradually move toward more complicated ones. This gives a clear picture as to what changes in the model results can be attributed to what changes in settings. The various experiments we did are summarized in Table 1.

The first experiment uses RAS with specified constant surface sensible and latent heat fluxes of 15.45 W/m^2 and 154.55 W/m^2 respectively, and a constant radiative cooling rate of 1.5 °C/day below 100 hPa, which reduces linearly in pressure to zero above 100 hPa. The rate of energy depletion due to the rate of radiative cooling exactly balances the rate of energy input due to the sum of the rates of surface heat flux. The model's own radiation package is not used in this experiment. The model's turbulent and boundary layer (including surface fluxes) computations are allowed to operate unmodified; but after each model physics step, the differences between the model-computed surface heat fluxes and the specified constant surface heat fluxes are used to uniformly modify the temperature and moisture of the bottom four levels, which reside in the boundary layer. This effectively fixes the surface fluxes at the preset values. Although the sea surface temperature is specified at 29 °C to allow the model computation to proceed, it does not affect the surface heat fluxes. The initial conditions are taken from a typical tropical sounding.

Under these horizontally uniform forcings, results averaged with respect to time and longitude are expected to be symmetric with respect to the equator since the model has a non-uniform Coriolis parameter (exceptions can occur, as will be discussed). Therefore, if the zonally-averaged precipitation varies with latitude, there should be either a maximum or a minimum in time- and zonally averaged precipitation at the equator: i.e., either a single ITCZ over the equator or a double ITCZ straddling the equator. Thus, the questions are, what are the forcings acting on the ITCZ, and how do they act to attract the ITCZ towards the equator or repel it away from the equator?

Figure 4 shows the zonally averaged precipitation, averaged between day 630 and day 730 of this experiment. This figure reveals a prominent latitudinal variation with one of the peaks at the equator, which may be referred to as an ITCZ. In another experiment with identical settings except that the Coriolis parameter is set to zero, the same field shows no distinct ITCZ structure (the solid line in Fig. 5). (Figures 4 and 5 show grid size variation in the polar regions. This is due to the polar filter employed in the model to allow normal-sized time steps in the presence of a reduced zonal grid size toward the poles.) This may lead to the conclusion that the Coriolis force is responsible for the existence of the ITCZ structure. However, the mere presence of the Coriolis force is not enough; the variation of the Coriolis parameter in latitude, i.e., β, is more important. Hence, an experiment with a constant Coriolis parameter (its value at 45°N) applied globally yields no ITCZ structure (the dashed line in Fig. 5).

Specified constant surface fluxes with a zero or uniform Coriolis parameter render all locations identical; therefore no latitudinal

Table 1 Summary of experiments

Figure	*Sfc*Flux	Radiation	Rotation	Convective trigger	Imposed symmetry
4	*C*	*C*	$f(\phi)$	*N*	*N*
5solid	*C*	*C*	$f(0)$	*N*	*N*
5dashed	*C*	*C*	$f(45)$	*N*	*N*
6	*I*	*C*	$f(\phi)$	*N*	*N*
7	*C*	*I-nc*	$f(\phi)$	*N*	*N*
8	*I*	*I-nc*	$f(\phi)$	*N*	*N*
9	*I*	*I-c*	$f(\phi)$	*N*	*N*
10	*I*	*I-nc*	$f(\ \phi)$	*N*	*Y*
12	*I*($ws = 5$)	*I-nc*	$f(\phi)$	*N*	*N*
13	*I*	*I-nc*	$f(\ \phi)$	*R95*	*N*

Where C = constant, I = Interactive, $f(\phi) = 2*\Omega*\sin(\phi)$, N = no, Y = yes, *R95* = relative humidity trigger function, *ws* = wind speed, and *nc* = no cloud-radiation interaction

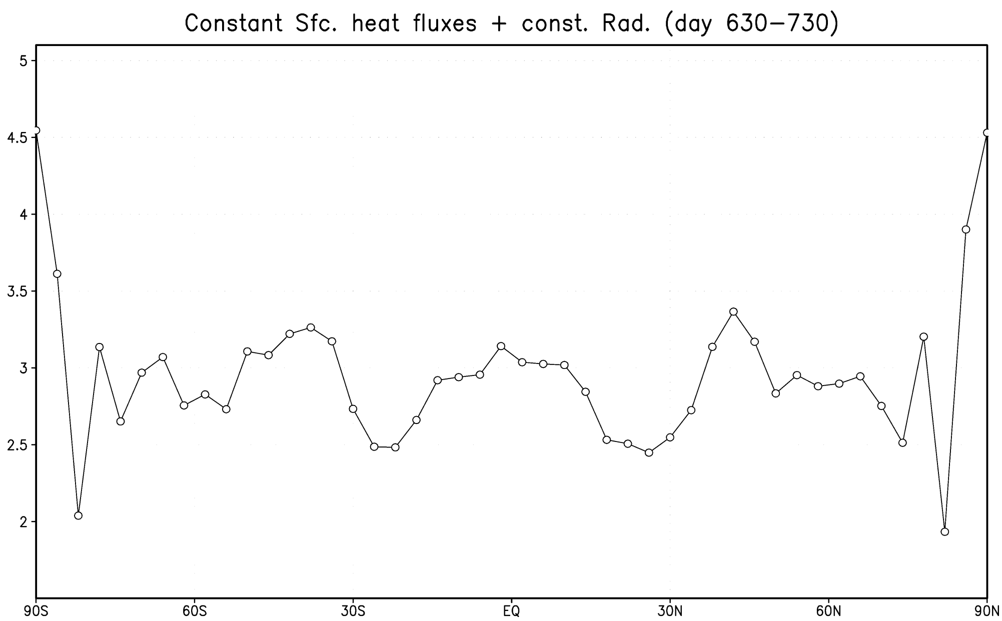

Fig. 4 The zonally averaged precipitation (mm/day) averaged between day 630 and day 730 of an experiment where the surface heat fluxes and the net radiative cooling rate are specified

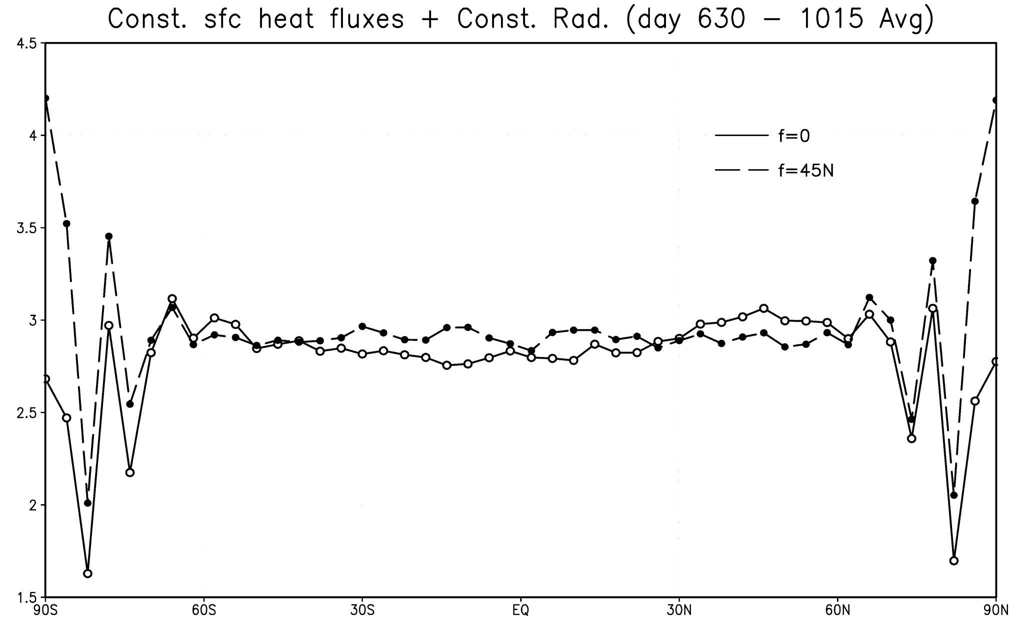

Fig. 5 Same as Fig. 4 except for experiments where *f* is specified as zero (*solid line*) and as its value at 45°N (*dashed line*)

variation in time and zonally-averaged precipitation can occur. [The slight difference between the tropics and the middle latitudes in the case of $f = 0$ (the solid line in Fig. 5) is likely due to a model design imperfection that is suppressed by the inertial stability provided by a non-zero uniform Coriolis parameter (f is that at 45°N, the dashed line in Fig. 5). A likely cause of this imperfection is that zonal grid size variation in the latitudinal direction is not recognized by the cumulus convection scheme.] In Fig. 4, the latitudinal variation is dominant in a range of about 40° to 60°. If the variation in this range is filtered out in this figure, the background distribution is remarkably uniform. These 40°- to 60°-size meridional cells can be considered predominantly as inertial gravity waves modified by β. An identical experiment using a zonally symmetric version of the model, which excludes any zonal waves, generated similar meridional cells. Thus, these cells are not maintained by interaction between mean flow and zonal waves.

The experimental fact that, as mentioned before, these cells owe their existence to β, can be explained by considering the frequency equation for inertial gravity waves. The squared frequency of the inertial gravity wave (in a rotating atmosphere with hydrostatic approximation):

$$\sigma^2 = f^2 + \alpha^2 N^2 + |F| \ , \qquad (1)$$

where

$$N^2 = (g\partial \ln \theta / \partial z)$$

turns negative. Equation (1) is from Eq. (8.4.23) of Gill (1982). In Eq. (1), f is the Coriolis parameter, g is the gravitational constant, α is the ratio of horizontal to vertical wave numbers, and θ is the potential temperature for a dry or unsaturated atmosphere and is the equivalent potential temperature when the atmosphere is saturated. $\partial\theta/\partial z$ is the vertical stability. A positive $|F|$ term is added in Eq. (1) to represent the effect of friction. Vertical stability is, of course, maintained by dynamical and physical processes that include radiative cooling, surface fluxes, and convective heating. For present purposes, it is only necessary to point out that a convective system occurs when the vertical instability (responsible for the synoptic systems) is large enough to overcome the stabilizing effects of rotation (i.e., the f^2 term) and friction. Thus, the definition of N, given already, should give way to a definition which is suitable for the release of latent heating in a cumulus convection scheme. Hence, when RAS is used, N^2 becomes negative when the cloud work function for at least one cloud type is greater than the corresponding critical cloud work function. Because it is linked to a cumulus convection scheme, the new N^2 has no simple analytic expression. With horizontally uniform surface fluxes and radiative cooling rate profile, the basic setting supports a horizontally-uniform N^2 basic state. With its minimal f, the equator is obviously a preferred location for convective activity. Such a preference is responsible for the existence of the meridional cells.

When surface heat fluxes are no longer fixed at constant values but are computed by the model's original design, and the globally-uniform radiative cooling vertical profile is retained and the sea surface temperature is set at a constant 29 °C, the ITCZ structure remains a single ITCZ over the equator (Fig. 6). In this instance, the globally averaged precipitation is somewhat higher than in the previous experiment (Fig. 4.) This is because the surface latent heat flux grows larger and the surface sensible heat flux grows smaller. (The total surface heat flux remains unchanged, since the radiative cooling has not changed.) This simply means that the Bowen ratio determined by the model is different from the one prescribed in the experiment with fixed surface fluxes. Figure 6 indicates that switching to the model's own surface fluxes yields a more vigorous variation in zonally averaged precipitation. The single ITCZ at the equator, however, remains.

The next experiment retains the constant specified surface heat fluxes but allows the model's own radiation package to operate, sans the radiation-cloudiness interaction, i.e., the cloudiness factor is set to zero. The solar angle is globally-uniform and is set at a value $Z1$, where $\cos(Z1)$ is equal to the globally averaged $\cos Z$, Z is the solar zenith angle, and $\cos Z$ is set to zero if it is negative. There is no distinct ITCZ structure in this instance (Fig. 7). When the model's own surface fluxes and radiative rates are used, again, without the radiation-cloudiness interaction and with a constant solar angle, a prominent ITCZ appears away from the equator (Fig. 8). When the radiation-cloudiness feedback in the model is allowed to operate, the result is not too dissimilar (Fig. 9). These experiments indicate that models' own surface fluxes allow a more prominent ITCZ; but it is the joint effect of the interaction between convection and radiation and the interaction between convection and surface fluxes that is most important in yielding a prominent off-equatorial ITCZ. When the experiment that corresponds to Fig. 8 was repeated with forced symmetry with respect to the equator, by replacing all prognostic quantities by the average over the North and South Hemispheres after each time step (i.e., each hemisphere is the mirror image of the other), the result is a prominent double ITCZ (Fig. 10). Apparently, the double ITCZ structure is less stable than the single ITCZ away from the equator. The reason for this remains to be explored.

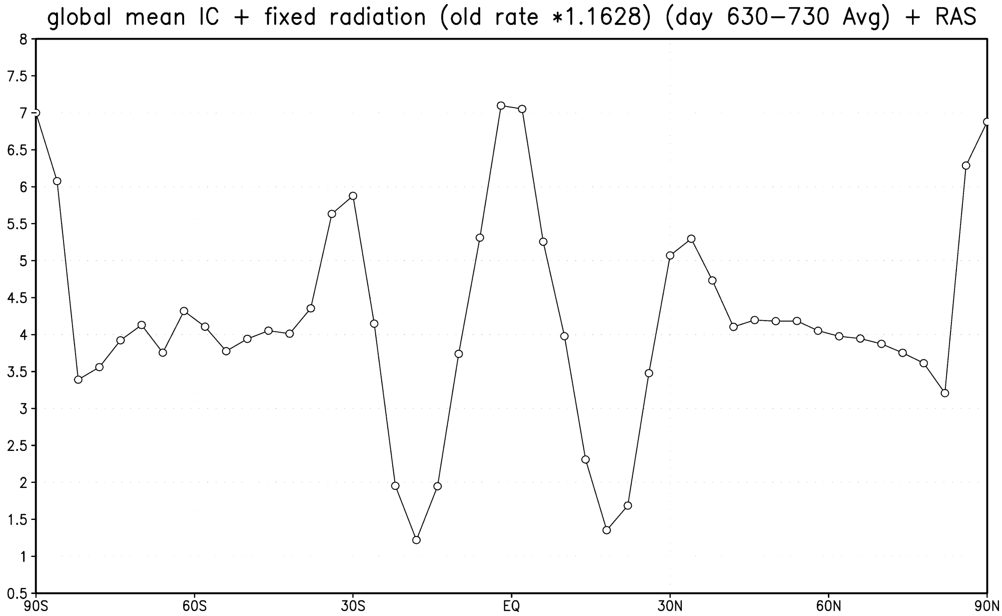

Fig. 6 The zonally averaged precipitation averaged between day 630 and day 730 of an experiment where the model's own surface heat fluxes and a specified net radiative cooling are used

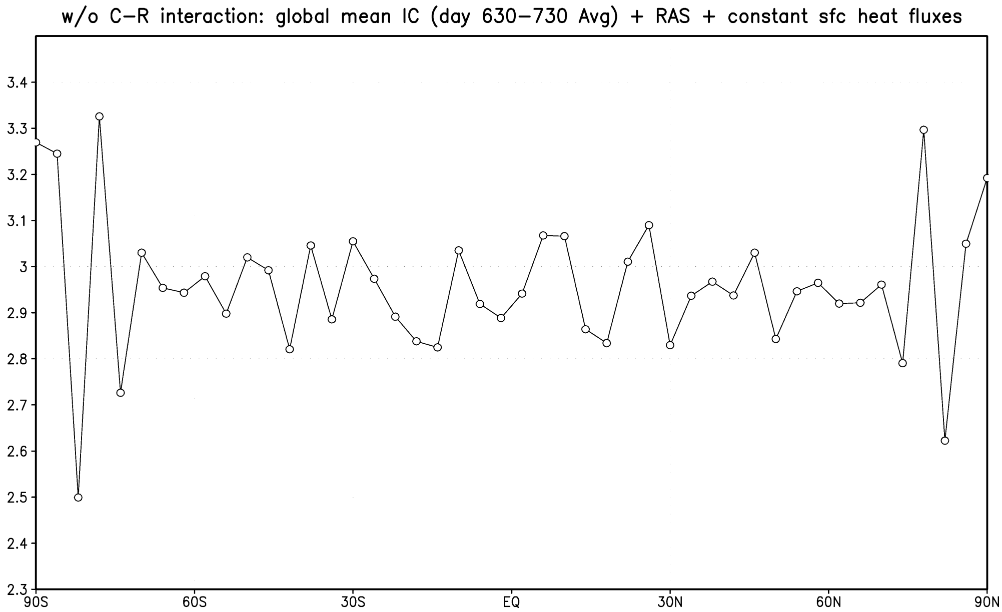

Fig. 7 The zonally averaged precipitation averaged between day 630 and day 730 of an experiment where specified surface heat fluxes and model's own radiation package are used

That the model's own surface fluxes yield more prominent ITCZ's (Fig. 6) can be understood as follows. The interaction between convection and surface fluxes is expected to generate more vigorous convective circulation. Convection is allowed to enhance surface fluxes right in its neighborhood, and thus there is a feedback between convection and surface fluxes. The end result is a more prominent meridional cell or stronger ITCZ. Our experiment does not yield a double ITCZ as a result of allowing interaction between convection and surface fluxes (i.e., the experiment represented by Fig. 6). This does not necessarily mean that such interaction yields a forcing pushing the ITCZ toward the equator. This forcing could still be pushing the ITCZ away from the equator but is not large enough to overcome the equator-ward forcing due to inertial stability (which is the first effect of Earth's rotation, as explained in CC01). That this forcing should push the ITCZ away from the equator can be understood by comparing the boundary layer flow near a convective center in the non-rotational and rotational cases (Fig. 11). In Fig. 11, when f is zero, the converging boundary air moves directly towards the convective center, and when f is not zero, the converging boundary layer air moves in a spiraling path with higher speed (due to the presence of the tangential wind), resulting in more evaporation and a greater moisture supply for the convection. Thus, the interaction between convection and surface fluxes has a tendency to move the ITCZ away from the equator.

That adding the interaction between convection and radiation (without cloud-radiation interaction) to the interaction between convection and surface fluxes is able to move the ITCZ away from the equator (Fig. 8) is explained as follows. When the model's radiation package is used there is greater radiative cooling outside of the ITCZ than inside the ITCZ due to the low humidity there. Therefore, outside of the ITCZ the model-resolved downward vertical motion has to become stronger to create more warming to balance the extra radiative cooling. Exactly the opposite occurs within the ITCZ. In other words, the "Hadley" circulation becomes stronger, which implies stronger surface winds which converge

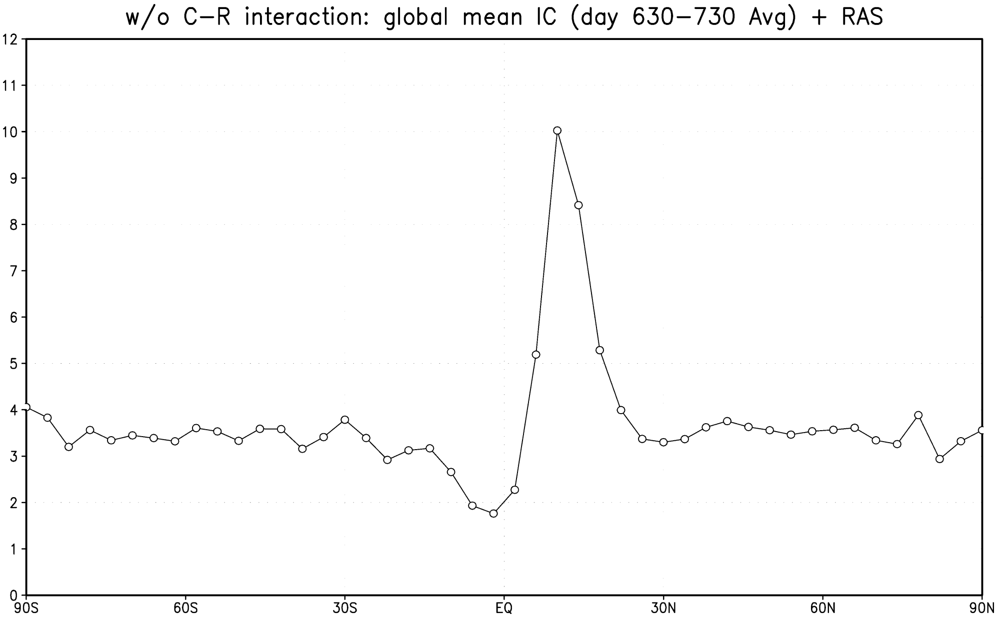

Fig. 8 The zonally averaged precipitation averaged between day 630 and day 730 of an experiment using the model's own surface heat fluxes and radiation package (but without cloudiness-radiation interaction) were used

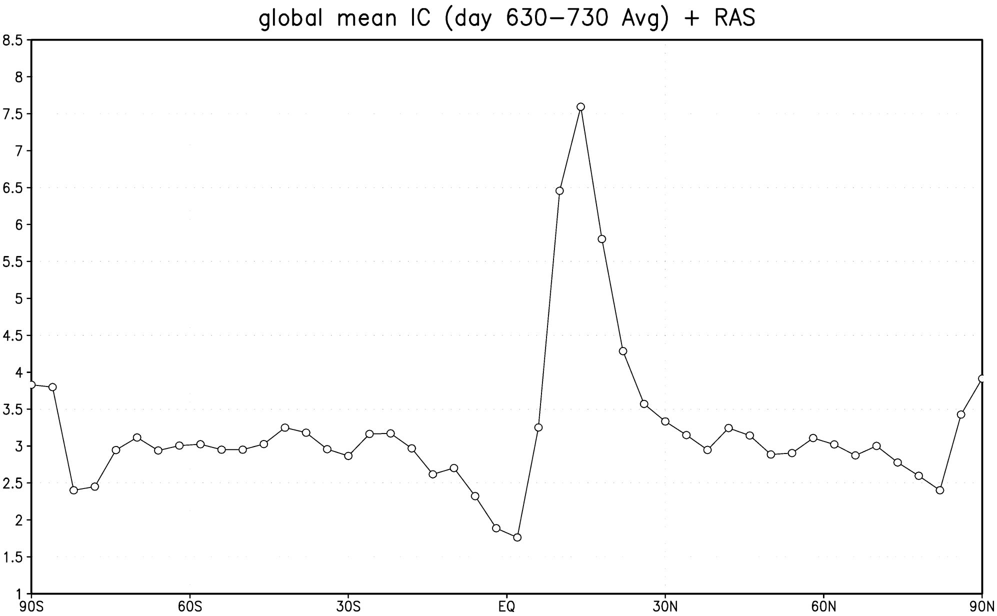

Fig. 9 Same as Fig. 8 except that the cloudiness-radiation interaction is allowed

toward the convective cells in the ITCZ. Therefore the surface fluxes become strong; that is, the second effect of rotation is larger. This results in moving the ITCZ away from the equator.

Note that only in the case when the model's own radiation and surface fluxes are used, the meridional cell takes on a global scale. In all other cases, the meridional cells are smaller and there are several of them.

The tendency to move the ITCZ away from the equator due to the interaction between convection and surface fluxes, which is enhanced by the convection-radiation interaction, sis related to the wind-evaporation feedback. By cutting off the wind-evaporation feedback, this tendency can be substantially reduced. Figure 12 shows the zonal-averaged precipitation over time for an experiment identical to that represented in Fig. 8, using the model's own radiation and surface heat fluxes, except that surface wind speed is replaced by a constant of 5 m/s in the surface heat fluxes computation. (Note that the globally averaged precipitation is higher than in the experiment represented in Fig. 8, indicating that the specified 5 m/s is too high.) Figure 12 shows a single ITCZ over the equator in this experiment, indicating that the tendency to move the ITCZ away from the equator due to the interaction between convection and surface fluxes is reduced by cutting off the wind-evaporation feedback.

When the boundary layer relative humidity is required to be greater than 95% before convection is allowed to occur, and this condition is applied to RAS, the experiment with model's own surface fluxes and radiation yields an ITCZ over the equator (Fig. 13). The explanation is as follows. Figure 14 shows the ratio of the magnitude of the Coriolis force to that of the pressure gradient force (CP ratio) at the bottom level of day 700 hour 0 for experiments with and without the condition that the boundary layer relative humidity must be $>95\%$ before convection is allowed to occur, with uniform f equal to that at 10N applied globally. The CP ratio is a measure of geostrophy, and is also a rough measure of the degree to which the spiraling effect of the Coriolis force is realized. With the $>95\%$ relative humidity condition, the CP ratio

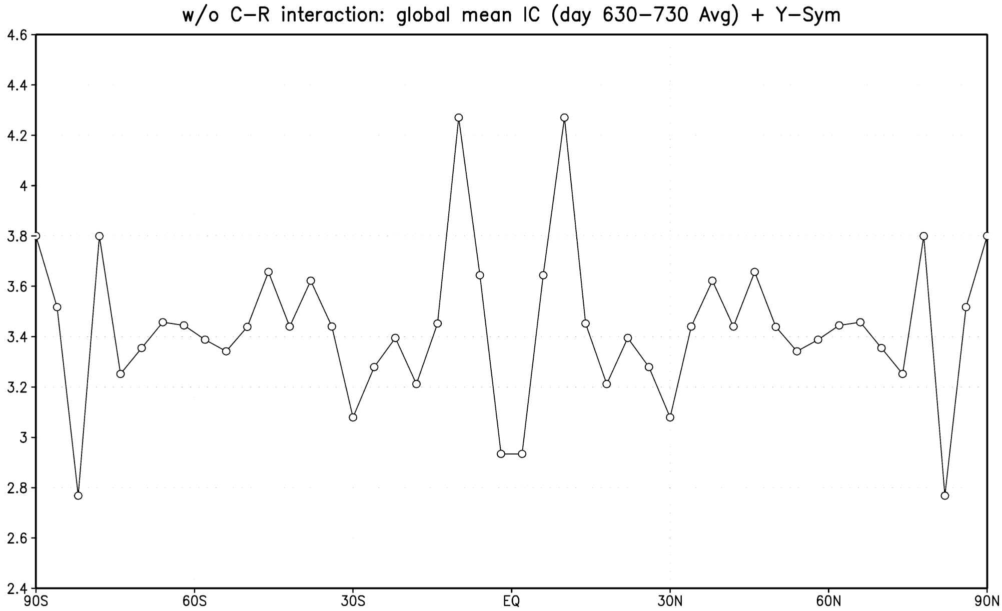

Fig. 10 Same as Fig. 8 except that the symmetry with respect to the equator is imposed

is smaller. This means that the convection-surface fluxes interaction is smaller due to the shorter time period for the Coriolis force to act on the air of the boundary layer to enable it to take on a spiraling path. This is the average time period between the time an air parcel moves downward to the boundary layer in the down-draft surrounding the convective center and the time the same air parcel moves upward in the convective center from the boundary layer. With the 95% relative humidity condition, the CP ratio is smaller because conditions are more stringent for convection to occur, but when it does occur, it is more vigorous, giving the boundary layer flow less time to be affected by the Coriolis force. In effect, the pressure gradient force surrounding the convective center is larger, resulting in a smaller CP ratio. Thus, with the 95% relative humidity condition, the convection-surface fluxes interaction becomes weaker. Therefore, the forcing that pushes the ITCZ away from the equator becomes smaller than the inertial stability forcing that pushes the ITCZ toward the equator. The result is a single ITCZ over the equator.

3 A hypothesis

The previous section cited a hypothesis that involves two types of forcing on the ITCZ, one pushing the ITCZ towards the equator and the other away from it. Yet, this hypothesis can only explain whether the ITCZ is over the equator or not. The fact that the ITCZ in Fig. 8 resides around 14°N instead of the middle or high latitudes needs additional explanation. The following hypothesis is offered to explain this and other results.

The two types of effects of the Earth's rotation acting on the ITCZ can be viewed as two attractors pulling on the ITCZ. The strength of the two types of attraction, or forcing acting on the ITCZ, is depicted schematically in Fig. 15. Curve A depicts the strength of the first attraction, or forcing acting on the ITCZ, which corresponds to the first term on the right hand side of Eq. (1). A positive value denotes southward attraction or forcing. Curve A is zero at the equator, since the equator is the center of the attractor. (The strength of an attraction

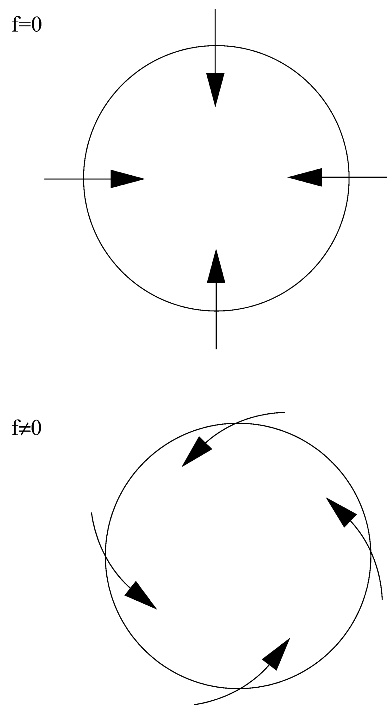

Fig. 11 Schematic diagram showing the effect of rotation on the boundary layer flow

at the center of an attractor is by definition zero.) The analytic form of curve A will be set forth below.

Curve B is the strength of the attraction due to the second effect of Earth's rotation, which corresponds to the second term on the right hand side of Eq. (1). Here, a positive value denotes northward attraction. Curve B is related to the interaction between convection and surface fluxes, mentioned in the previous section with respect to Fig. 11. Because it is related to the thermodynamics and circulation of the model atmosphere,

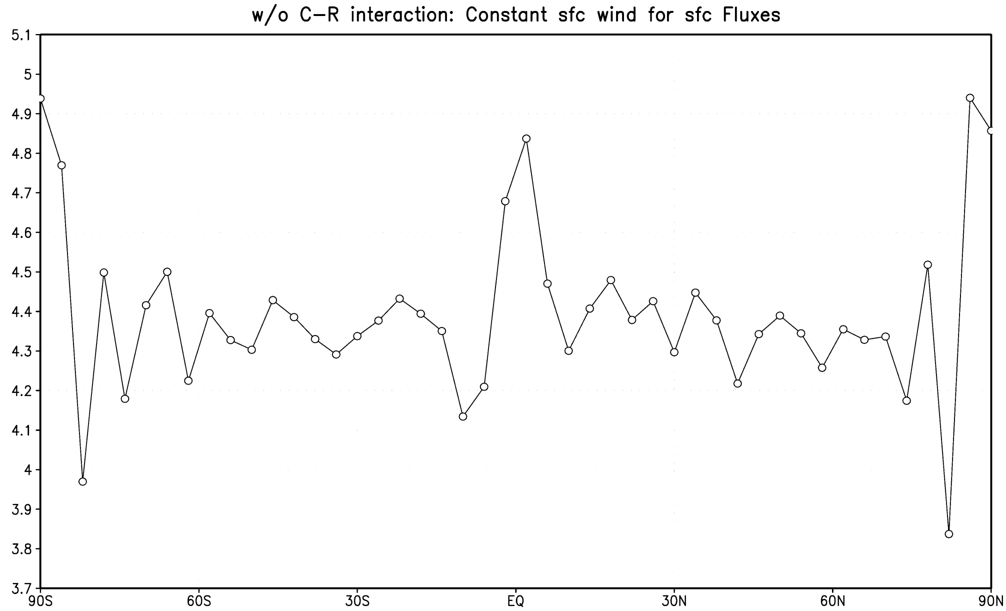

Fig. 12 Same as Fig. 8 except that in the computation of surface heat fluxes a constant 5 m/s wind speed, instead of model's own surface wind, is used

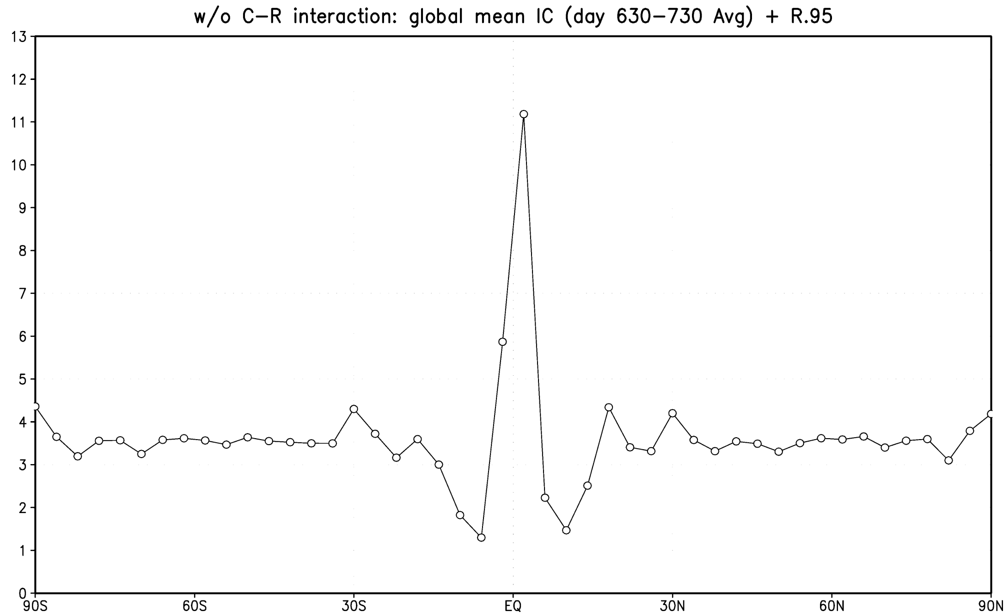

Fig. 13 Same as Fig. 8 except that a condition of relative humidity in the boundary layer is larger than 95% in imposed on RAS

curve B depends on the choice of the cumulus parametrization scheme, whereas curve A does not. There is no analytic expression for curve B, whose shape is obtained through qualitative arguments only. Like the f^2 term, the $|F|$ term is positive and has a stabilizing effect. In Fig. 15, the effect of the $|F|$ term has been incorporated into curve B to give curve B a somewhat smaller magnitude. Both curve A and curve B are anti-symmetric with respect to the equator; thus, only the picture in the Northern Hemisphere is set forth.

Due to the effects of radiative cooling and a fixed SST, convection must occur in the model; i.e., $\sigma^2 < 0$ is expected to be satisfied within a certain latitudinal range. Thus, the strongest convection should occur where σ^2 is a minimum. Therefore, the latitude of the ITCZ can be identified as the latitude where $\partial\sigma^2/\partial\phi = 0$. Consequently, the latitude of the ITCZ is where $\partial f^2/\partial\phi$ (curve A) is balanced by the latitudinal gradient of the second and third terms on the right hand side of Eq. (1) (curve B). The term $\partial f^2/\partial\phi$ is equal to 8 $\Omega^2 \sin\phi \cos\phi$, where Ω is Earth's rate of rotation and ϕ the latitude. Thus curve A is known analytically.

Since curve A, which is equal to 8 $\Omega^2 \sin\phi \cos\phi$, with a maximum at 45°N, is plotted in Fig. 15 only in a schematic way, it is only necessary to assert that curve A is zero at the equator, and first increases and then decreases northward until it reaches zero at the north pole. This assertion is reasonable in the sense that the strength of the attraction is supposed to be zero at the center of the attractor, i.e., the equator. Also, curve A should be

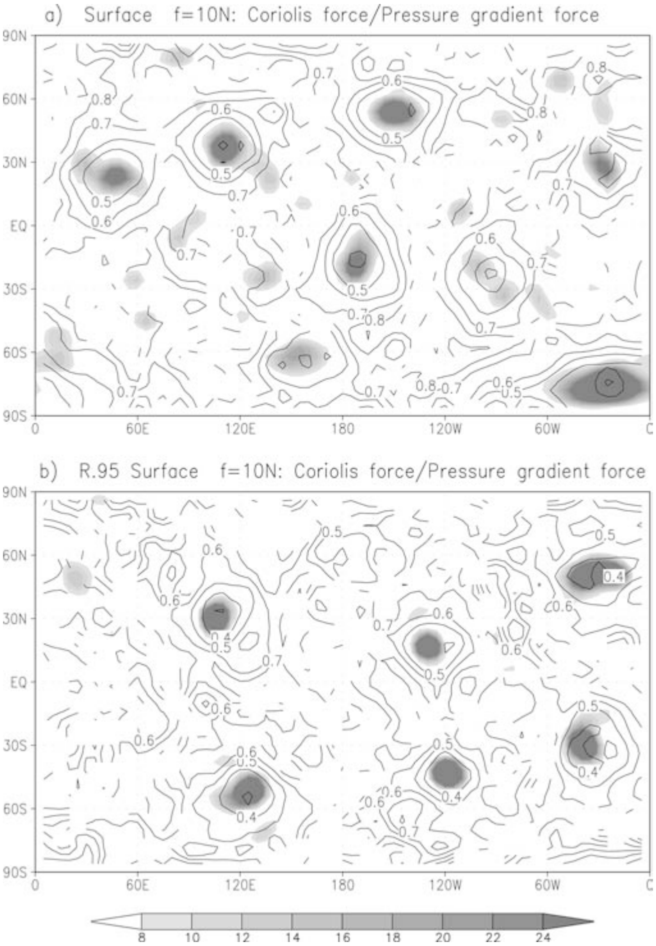

Fig. 14 Ratio of the magnitude of the Coriolis force to that of the pressure gradient force at the bottom level for experiments where f is specified globally uniform at its value at 10°N for cases and where the boundary layer relative humidity exceeds 95% condition is **a** not and **b** is imposed on RAS

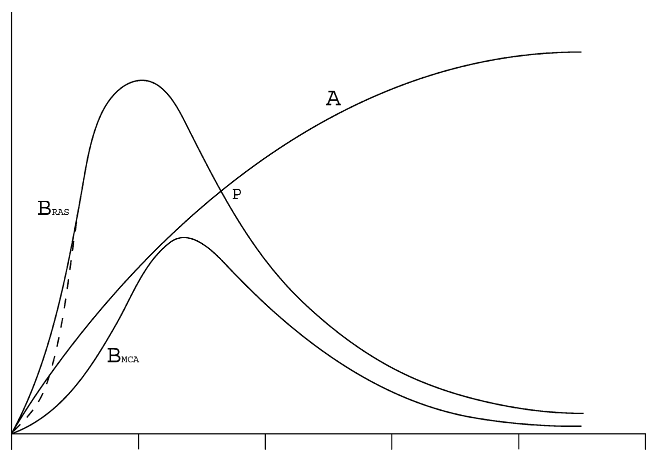

Fig. 15 Schematic diagram showing the strength of the two types of attraction acting on the ITCZ. The difference between *solid* and *dashed curve Bs* lies in the slope of *curve B* at the equator

zero at the north pole (an unstable equilibrium location) again, due to the symmetry there. In addition, it is necessary to assert that the slope of curve A at the equator is nonzero, according to the equation given for $\partial f^2/\partial\phi$.

As mentioned, curve B is related to the dependence of the second term on the right hand side of Eq. (1) on the Earth's rotation and is due to two attractors at the poles. Again, a positive value denotes northward forcing on the ITCZ. Thus, curve B is positive in the Northern Hemisphere, where the attraction is towards the north pole, but is zero at the north pole, which is the center of the attractor, and at the equator, due to symmetry. In Fig. 15, curve B has been drawn in a way that can best fit the experimental results. Why the peak of curve B is in the tropics instead of at the middle or high latitudes remains to be explained, and an explanation will be provided at the end of this section.

Also, in Fig. 15, a curve B has been plotted for each of RAS and MCA. Bras is larger than Bmca, and the reason will be discussed at the end of this section. The intersection of the two curves is where the ITCZ resides. For MCA, the intersection is at the equator, and for RAS, it is at the latitude of point P, according to Fig. 15. Since at the equator, the slope of curve A is different from that of curve B (which is nonzero), the equator can be a stable or an unstable equilibrium. For MCA, the equator is the only stable equilibrium. For RAS, the equator can also be a stable equilibrium only if the slope of curve A there is larger than that of curve B (the dashed curve in Fig. 15).

A stable ITCZ at the equator was obtained in an experiment using RAS with an earlier version of our model (Chao and Deng 1998, Fig. 3), along with two ITCZs straddling the equator. The fact that that version of the model had a peak SST at the equator might have helped the equatorial ITCZ to exist. Our experiments with RAS with the current version of the model have not yielded three concurrent ITCZs. Somehow, with RAS, the slope of curve A at the equator is smaller than that of curve B. The reason for that is not clear. It is possible that the equilibrium at the equator is weak and can easily be overwhelmed by one component of the double ITCZ in the same process that allows one component of the double ITCZ to suppress the other.

Figure 15 is supported by two experiments reported in CC01. Figure 2 (taken from CC01) shows the zonally averaged precipitation of an experiment using RAS. In that experiment, over the first 200 days, the relative humidity of the boundary layer was required to remain above 90% for any cumulus convection to occur. Over the next 100 days, the criterion was changed linearly from >90% to >95%. Thereafter, it remained at >95%, thus making RAS behave more like MCA. The SST was globally constant at 29 °C, and the solar angle remained uniform, with a value equal to that of its global mean. Results showed that the convection region moved from an off-equatorial position to the equator over a period of 30 days, starting from day 225. This corresponds to a diminution of curve B to below that of curve A, and the disappearance of the intersecting point, P.

Figure 3, also taken from CC01, shows the same experiment, except that the criteria of 90% and 95% are switched. (In the 95% time domain, there are precipitation peaks at around 25°N & S, but they are intermittent and not prominent in the time-mean sense. See Fig. 7 of CC01.) The shift of the convection region away from the equator around day 252 is rather abrupt. This corresponds to the fact that when the slope of curve B at the equator surpasses that of curve A, the peak of curve B already exceeds curve A by a large amount. This large difference means that the attraction pulling the ITCZ away from the equator is very large, resulting in the abrupt shift of the ITCZ away from the equator. This difference is much smaller in the other case.

In Fig. 15, curve Bmca represents the situation when MCA replaces RAS. It also represents the situation when the 95% criterion is applied to RAS. The difference between curves A and B in Fig. 15 yields the net attraction due to Earth's rotation. For both RAS and MCA, the net attraction is zero at the equator. With positive values representing a southward attraction, for RAS, the net attraction decreases with latitude initially, but increases back to zero at around 16°N. For MCA, the net attraction *increases* with latitude initially, but then drops to almost zero at 16°N, and increases after that. These are the results found experimentally in Chao (2000, curve A of his Fig. 8).

In Fig. 15 curve B has been plotted individually for both RAS and MCA (or, RAS with the 95% relative humidity condition). Bras is larger than Bmca, because MCA has a more stringent criterion for convection to occur, i.e., the relative humidity must be 100%. Thus, with MCA, when convection does occur, it is more intense and concentrated in a smaller area. Higher intensity and concentration reduce the chances that the convective circulation will pick up moisture at the surface. This has been discussed in the previous section in association with Fig. 14.

As stated, the peak of curve B is in the tropics instead of in the higher latitudes. A qualitative explanation can account for this. A convective system in the Northern Hemisphere, according to the definition of curve B, experiences attraction toward the north pole and this attraction is related to the gradient of f; thus the attraction increases toward the equator. However, close to the equator, due to the large size of the convective system, part of the system covers a domain south of the equator and thus experiences attraction from the attractor at the south pole. At the equator, the attractions due to both poles cancel and curve B should be zero. This is illustrated in Fig. 16, where curve B is the latitudinal running mean of the dashed curves, which represent the magnitude of the attraction toward the poles, and the running mean uses a window the size of the synoptic system. Therefore, curve B has a peak close to the equator.

4 Discussion

A fundamental difference between our interpretation and that of the previous theories mentioned in the Appendix is that the attraction represented by curve B in our theory is not present in the previous theories. The dependence of curve B on the cumulus scheme is a cornerstone of our interpretation of the dependence or the latitudinal location of the ITCZ on the cumulus scheme. This cornerstone involves how the cumulus scheme affects surface heat flux, and this is what is lacking in the previous theories.

Factors affecting the cumulus scheme may or may not affect the ITCZ. For example, Sumi's (1992) results showed that a single ITCZ over the equator could turn

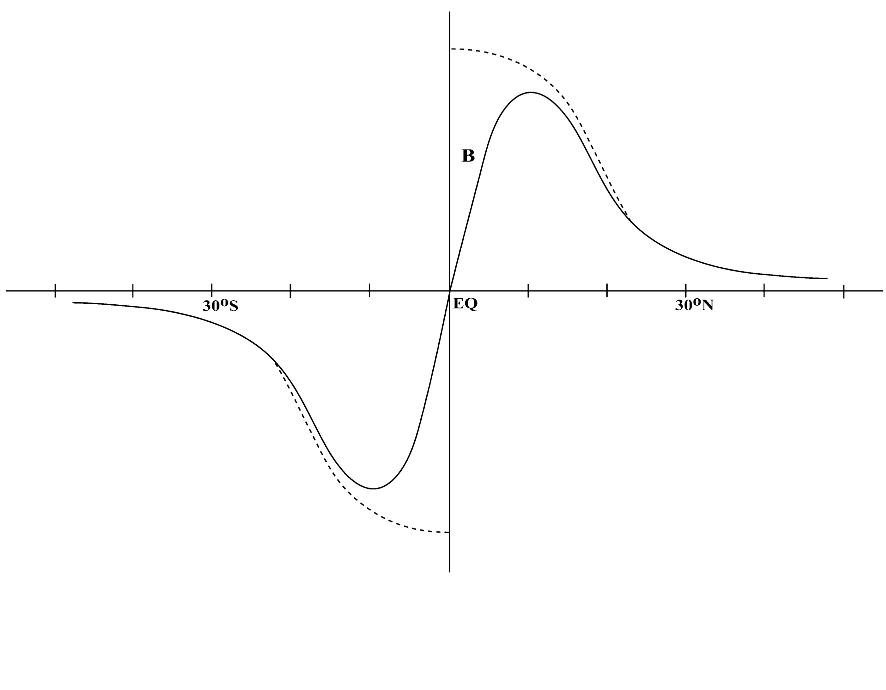

Fig. 16 Schematic diagram showing *curve B* as the running average of the magnitude of the attraction toward the poles

into a double ITCZ when the horizontal resolution of the model is doubled. His interpretation was that the low-resolution model could not resolve the double ITCZ. However, there could be other considerations, such as the impact of resolution on cumulus convection. In this regard, cumulus convection becomes more intense when grid size is reduced, due to the fact that larger convergence is more likely to occur as the grid becomes smaller. Thus, when the horizontal resolution is changed, the cumulus convection scheme is effectively changed. In other words, the grid size is a part of a cumulus convection scheme, and how to incorporate grid size into a cumulus convection scheme is an important research direction (Jung and Arakawa 2004), (and how grid size influences the latitudinal location of the ITCZ is an important research direction).

On the other hand, an experiment we did in which the SST remained spatially uniform, but where temperature increased from 29 °C to 32 °C over 400 days, the latitudinal location of the ITCZ did not change systematically, aside from some short-term (∼2-week) fluctuations. Thus, it appears that temperature of the SST can be ruled out as a significant influence on latitudinal location of the ITCZ under the U-SST-SA conditions.

Surface friction, though, has a damping effect on convection, and thus can affect the latitudinal location of the ITCZ. The effect of surface friction is represented as a part of the positive term $|F|$ on the right-hand side of Eq. (1), the other part being internal friction. Thus, curve B in Fig. 15 can be considered as representing both friction and the second effect of the Earth's rotation. When friction is removed, curve B rises somewhat. This will result in a poleward movement of the ITCZ. An experiment in which the coefficient of surface friction is multiplied by a factor of 2 in the first 100 days, and is reduced to zero over the next 400 days, indeed shows a slight poleward movement of the ITCZ (figure not shown). Internal friction is expected to have a similar, though lesser, effect.

Sometimes, one component of a double ITCZ does not appear, resulting in one ITCZ away from the equator, as mentioned earlier, and as shown in Figs. 8 and 9. Whether this has something to do with some element(s) of the cumulus convection scheme or not is yet to be explained.

The latitudinal dependence of α in Eq. 1 has not been touched upon. Since a spectrum of gravity waves is excited, α is not a single value, but it does have a dominant value. How this dominant value depends on latitude is not yet understood.

The differences between the results of our model and those of Sumi (1992) and Kirtman and Schneider (2000), as mentioned in the Introduction, indicate that there are other important factors (influencing the latitudinal location of the ITCZ) besides the cumulus convection scheme. The identities and interpretation of these factors remain to be studied.

5 Summary

Previous experimental studies have found that through one of several model design changes, the ITCZ structure in an aqua-planet model with globally and temporally uniform SST and solar insolation angle can switch between a single ITCZ over the equator and a double ITCZ straddling the equator. In the latter case, one component of the double ITCZ may be absent, leaving one ITCZ away from the equator. These model design changes include switching to a different cumulus parametrization scheme, changes in the cumulus parametrization schemes, and changes in the horizontal resolution. Difficulties encountered by the previous theories of ITCZ in explaining these findings are discussed in the Appendix.

Here, an interpretation has been offered for these findings, based on the balance between two types of attraction on the ITCZ, both due to the Earth's rotation. The first type attracts the ITCZ towards the equator, and is independent of the cumulus parametrization scheme. The second type repels the ITCZ away from equator, and is dependent on the on the cumulus parametrization scheme. The first type is related to the inertial stability. The second type is related to the interaction between convection and surface fluxes, and is enhanced by the interaction between convection and radiation. The balance between the two types of attraction can change as the model design is changed, thus resulting in a switch between a single ITCZ and a double ITCZ.

Acknowledgements The authors thank Dr. H. Mark Helfand for help in using his PBL parametrization. Kay E. Cheney improved the writing. This work was supported by NASA Office of Earth Science.

6 Appendix 1

6.1 Difficulties with previous theories of the latitudinal location of the ITCZ

The experimental findings enumerated in the Introduction present a good means to test the various theories of the latitudinal location of the ITCZ. Waliser and Somerville (1994) and Tomas and Webster (1997) have reviewed these theories. For example, Charney's (1971) explanation for the latitudinal location of the ITCZ involves a balance of two components. One component is the efficiency of Ekman pumping (or frictionally induced low-level convergence), which favors a larger Coriolis parameter or location at the poles. The other component is the higher moisture content (or temperature) of the tropics, which favors a location at the equator. The second component does not exist under U-SST-SA conditions, therefore Charney's (1971) explanation results in ITCZs at the poles under these conditions, in contradiction to our model results. Hence, one must conclude that Charney's (1971) first component is either incorrect or incomplete. His first component is essentially derived from a zonally symmetric version of the conditional instability of the second kind (CISK) theory for tropical cyclogenesis. The exact theoretical reason(s) for failings of the CISK theory is still not a settled question, although some very persuasive discussions have been presented (Emanuel et al. 1994).

Holton et al. (1971) also based their theory to explain the latitudinal location of ITCZs on the efficiency of Ekman pumping. Instead of using zonal symmetry, they considered the fact that the ITCZs consist of many propagating synoptic waves. Their conclusion was that the Doppler-shifted frequency of the synoptic waves is equal to the Coriolis parameter. However, as pointed out by Lindzen (1974) regarding diurnal oscillation, there is no observational evidence of maximum precipitation intensity at 30° latitude, as predicted by Holton et al. (1971). Moreover, Holton et al. (1971) imply that at any latitude, there can only be one wave frequency. Observations, however, show that an ITCZ contains more than one wave frequency (Takayabu et al. 1996, their Fig. 3). Also, just as with Charney (1971) theory, the fact that under U-SST-SA conditions, switching cumulus convection schemes leads to switching locations by the ITCZ, cannot be explained by Holton et al. (1971), whose theory is not sensitive to different cumulus convection schemes.

Waliser and Somerville (1994) theory is also built on frictionally induced low-level convergence, and it has no provision to account for the dependence of the latitudinal location of the ITCZ on the cumulus convection scheme, either.

Lindzen (1974) wave-CISK theory, first discussed by Hayashi (1970, 1971), does not rely on Ekman pumping (or frictionally induced low-level convergence), but there is also no provision to account for the dependence of the ITCZ latitudinal location on the cumulus convection scheme.

Tomas et al. (1999) work, is an extension of that of Tomas and Webster (1997), and emphasizes the role of the cross-equatorial surface pressure gradient in determining the latitudinal location of the ITCZ. Although they realized from observations that there are two modes of ITCZ latitudinal locations (equatorial and off-equatorial), which correspond to different magnitudes of the cross equatorial surface pressure gradient, how these two modes arise is not explained. Since the cross-equatorial surface pressure gradient is a model-produced quantity, and cannot be specified externally, their model, which is relaxed to a specified cross-equatorial surface pressure gradient, does not lead to a self-contained theory to account for the latitudinal location of the ITCZ. Also, their article does not discuss the sensitivity of ITCZ location to the cumulus convection scheme.

In summary, the theories described here, when applied to U-SST-SA conditions, do not explain or predict the dependence of the latitudinal location of the ITCZ on the cumulus convection scheme. Other theories of the ITCZ, such as those of Xie and Saito (2001) and Philander et al. (1996), invoke continental distribution and ocean–atmosphere interaction, respectively, and are thus not applicable to the problem at hand.

References

Chao WC (2000) Multiple quasi-equilibria of the ITCZ and the origin of monsoon onset. J Atmos Sci 57: 641–651

Chao WC, Chen B (2001a) Multiple quasi-equilibria of the ITCZ and the origin of monsoon onset. Part II. Rotational ITCZ attractors. J Atmos Sci 58: 2820–2831

Chao WC, Chen B (2001b) The role of surface friction in tropical intraseasonal oscillation. Mon Weather Rev 129: 896–904

Chao WC, Deng L (1998) Tropical intraseasonal oscillation, super cloud clusters and cumulus convection schemes. Part II. 3D Aqua-planet simulations. J Atmos Sci 55: 690–709

Charney JG (1971) Tropical cyclogenesis and the formation of the ITCZ. In: Reid WH (ed) Mathematical problems of geophysical fluid dynamics. Lectures in applied mathematics. Am Math Soc 13: 355–368

Emanuel KA, Neelin JD, Bretherton CS (1994) On large-scale circulations in convecting atmosphere. Q J R Meteorol Soc 120: 1111–1145

Gill AE (1982) Atmosphere-ocean dynamics. Academic Press, San Diego, pp 662

Holton JR, Wallace JM, Young JA (1971) On boundary layer dynamics and the ITCZ. J Atmos Sci 28: 275–280

Hayashi Y (1970) A theory of large-scale equatorial waves generated by condensation heat and accelerating the zonal wind. J Meteorol Soc Japan 48:140–160

Hayashi Y (1971) Large-scale equatorial waves destabilized by convective heating in the presence of surface friction. J Meteorol Soc Japan 49: 458–465

Hess PG, Battisti DS, Rasch PJ (1993) Maintenance of the intertropical convergence zones and the tropical circulation on a water-covered earth. J Atmos Sci 50: 691–713

Jung JH, Arakawa A (2004) The resolution dependence of model physics: Illustration from nonhydrostatic model experiments. J Atmos Sci 61:88–102

Kirtman BP, Schneider EK (2000) A spontaneously generated tropical atmospheric general circulation. J Atmos Sci 57: 2080–2093

Kuo HL (1965) On the formation and intensification of tropical cyclones through latent heat release by cumulus convection. J Atmos Sci 22: 40–63

Lindzen RS (1974) Wave-CISK in the tropics. J Atmos Sci 31: 156–179

Manabe S, Smagorinsky J, Strickler RF (1965) Simulated climatology of a general circulation model with a hydrological cycle. Mon Weather Rev 93: 769–798

Moorthi S, Suarez MJ (1992) Relaxed Arakawa-Schubert: a parametrization of moist convection for general circulation models. Mon Weather Rev 120: 978–1002

Philander SGH, Gu D, Halpern D, GLambert G, Lau NC, Li T, Pacanowski RC (1996) Why the ITCZ is mostly north of the equator. J Clim 9: 2958–2972

Sumi A (1992) Pattern formation of convective activity over the aqua-planet with globally uniform sea surface temperature. J Meteorol Soc Japan 70: 855–876

Tackacs LL, Molod A, Wang T (1994) Documentations of the Goddard Earth Observing System (GEOS) General Circulation Model-Version 1. NASA Technical Memovandum 104606 vol. 1, Goddard Space Flight Center, Greenbelt, MD 20771, USA, pp 97

Takayabu YN, Lau KM, Sui CH (1996) Observation of a quasi-2-day wave during TOGA COARE. Mon Weather Rev 124: 1892–1913

Tomas RA, Webster PJ (1997) The role of inertial instability in determining the location and strength of near-equatorial convection. Q J R Meteorol Soc 123: 1445–1482

Tomas RA, Holton JR, Webster PJ (1999) The influence of cross-equatorial pressure gradients on the location of near-equatorial convection. Q J R Meteorol Soc 135: 1107–1127

Waliser DE, Somerville RCJ (1994) Preferred latitude of the ITCZ. J Atmos Sci 51: 1619–1639

Xie SP, Saito K (2001) Formation and variability of a northerly ITCZ in a hybrid coupled AGCM: Continental forcing and oceanic-atmospheric feedback. J Clim 14: 1262–1276